Journal of Photochemistry and Photobiology A: Chemistry 199 (2008) 316–321

Contents lists available at ScienceDirect

Journal of Photochemistry and Photobiology A: Chemistry

journal homepage: www.elsevier.com/locate/jphotochem

# An annelated thioxanthone as a new Type II initiator

Demet Karaca Balta, Nihal Cetiner, Gokhan Temel, Zuhal Turgut, Nergis Arsu*

*Yildiz Technical University, Department of Chemistry, Davutpasa Campus, Istanbul 34210, Esenler, Turkey*

ARTICLE INFO

*Article history:*
Received 10 March 2008
Received in revised form 21 May 2008
Accepted 12 June 2008
Available online 21 June 2008

*Keywords:*
Photopolymerization
Thioxanthone
Type II initiator

ABSTRACT

5-Thia-naphthacen-12-one (TX-Np) was synthesized as a potential photoinitiator for radical polymerization. Polymerization studies revealed that TX-Np acts as a photoinitiator for radical polymerization of acrylic type monomers in the presence of *N*-methyldiethanolamine (MDEA). The phosphorescence spectrum measured at 77 K in ethanol showed an emission band at $\lambda_{max}$ = 505 nm corresponding to the approximate triplet energy of ca. 237 kJ/mol.

The phosphorescence lifetime was found to be 197 ms corresponding to a $\pi$–$\pi^*$ nature of the lowest triplet state. The quantum yield for fluorescence emission ($\phi_f$) in benzene was found to be 0.045. Spectroscopic and polymerization studies revealed that photoinitiation occurs through the $\alpha$-aminoalkyl radical, similar to thioxanthone-based photoinitiators. Since MDEA is required for TX-Np to act as an initiator for acrylate polymerization, it is suggested that the TX-Np reacts with MDEA to give $\alpha$-aminoalkyl radicals which initiate polymerization.



## 1. Introduction

Photoinitiators which are used to start a radical photoinduced polymerization reaction upon exposure to UV light have been known as playing one of the most important roles in reaching high conversions of the monomer [1]. Photoinitiated radical polymerization may be initiated by both $\alpha$-cleavage (Type I) and H-abstraction (Type II) initiators [2].

*Type II* photoinitiators are a second class of photoinitiators and are based on compounds whose triplet excited states are reacted with hydrogen donors thereby producing an initiating radical [3–5] (Scheme 1). Because the initiation is based on bimolecular reaction, they are generally slower than *Type I* photoinitiators which are based on unimolecular formation of radicals. On the other hand, *Type II* photoinitiators possess better optical absorption properties in the near-UV spectral region. Benzophenone (BP) and thioxanthone (TX) are well known Type II photoinitiators for the radiation curing of coatings, printing inks, etc. [6–9]. The large variety of Type II initiators allows radical reactions to be initiated by UV as well as visible light and are used extensively in heavily pigmented formulations as well as printing inks and wood coatings.

Among *Type II* photoinitiators, thioxanthone derivatives, in conjunction with tertiary amines, are efficient photoinitiators with absorption characteristics that compare favorably with benzophenone derivatives [10] and have been used for many years for curing formulations containing $TiO_2$. More recently, we have developed a new class of photoinitiator, namely thioxanthone–anthracene (TX–A) of the following structure (Scheme 2), exhibiting completely different photochemical behaviour than that of conventional TX type photoinitiators [15].

In contrast to the TX type of photoinitiators, this photoinitiator is an efficient photoinitiator for free radical polymerization of both acrylic and styrenic type monomers in the presence of oxygen without an additional hydrogen donor.

In this study, as a continuing interest [11–15] in synthesizing novel photoinitiators thioxanthone–naphthalene was synthesized and used as an initiator for the polymerization of acrylates and methacrylates. The initiation efficiency was determined in an air or nitrogen atmosphere and compared when an amine was added to the formulations.

## 2. Experimental

### 2.1. Materials

Thioxanthone–naphthalene was synthesized as described previously [16,17]. Naphthalene and thiosalicylic acid were obtained from Aldrich and used as received. *N*-methyldiethanolamine (MDEA, 99%, Aldrich) was used as received. Methyl methacrylate (MMA) (≥99%, Fluka) was washed with 5% aq. NaOH solution, dried over $CaCl_2$ and distilled over $CaH_2$ *in vacuo*. Dichloromethane ($CH_2Cl_2$) and benzene (Merck) were used as received. Trimethylolpropane triacrylate (95%, Aldrich) and Photomer-3038 (Cognis),

* Corresponding author. Tel.: +90 212 383 4186; fax: +90 212 383 4134.
*E-mail address:* narsu@yildiz.edu.tr (N. Arsu).

1010-6030/$ – see front matter © 2008 Elsevier B.V. All rights reserved.
doi:10.1016/j.jphotochem.2008.06.008

$$Ar_2C{=}O \xrightarrow{h\nu} {}^3[Ar_2C{=}O]^* \quad (1)$$

$${}^3[Ar_2C{=}O]^* + R\text{-}H \longrightarrow Ar_2\dot{C}\text{-}OH + R\bullet \quad (2)$$

$$R\bullet + \text{Monomer} \longrightarrow \text{Polymer} \quad (3)$$

**Scheme 1.** Photoinitiated free radical polymerization by using aromatic carbonyl compounds.

(a mixture of epoxyacrylate (75%) and tri(propylene glycol) diacrylate (TPGDA) (25%)) were used as received.

### 2.2. Synthesis of 5-thia-naphthacen-12-one (TX-Np)

Thiosalycylic acid (1.6 g, 0.010 mol) was slowly added to 15 mL of concentrated sulfuric acid, and the mixture was stirred for 5 min to ensure through mixing. Naphthalene (5.6 g, 0.044 mol) was added slowly to the stirred mixture over a period of 30 min. After the addition, the reaction mixture was stirred at room temperature for 1 h and then at 60 °C for 4 h, after which it was left to stand at room temperature overnight. The resulting mixture was poured carefully with stirring into a 10-fold excess of boiling water, and it was boiled for a further 5 min. The solution was cooled and filtered. The residue was recrystallized from dioxane–water (50:50). $m_p$: 180 °C.

Anal. Calcd. for $C_{17}H_{10}OS$ (262 g mol$^{-1}$): C, 77.83%; H, 3.84%; S, 12.22% Found: C, 77.71%; H, 3.11%; S, 12.56%.

$^1$H NMR (250 MHz) in DMSO: $\delta$ 8.52–8.43 (m, 4H, aromatic), 8.22–7.65 (m, 6H, aromatic).

IR(KBr):$\nu$ (cm$^{-1}$) 3457, 3056, 2921, 2852, 1631, 1617, 1438, 1387, 1211, 1161, 1033.

### 2.3. Photopolymerization

Appropriate solutions of the monomer and TX-Np in $CH_2Cl_2$ in the presence of *N*-methyldiethanolamine were irradiated in a photoreactor equipped with eight Philips black lamps emitting nominally at $\lambda$ = 350 nm for 60 min in an air atmosphere. Polymers were obtained after precipitation in methanol and drying *in vacuo*. Conversions were calculated for all samples gravimetrically.

### 2.4. Analyses

Photo-DSC experiments were done on a TA DSC 100 instrument and a TA Q PCA photo unit equipped with a high-pressure mercury lamp. Measurements were carried out in isothermal mode at 25 °C and under an inert atmosphere (nitrogen flow: 50 mL/min).

UV–vis spectra were taken on an Agilent 8453. IR spectra were recorded on an ATI Unicam Mattson 1000 FT/IR-3 spectrophotometer on a KBr disc.

Elemental analysis was performed on a CHNS-932 LECO instrument.

Fluorescence and phosphorescence spectra were recorded on a Jobin Yvon–Horiba Fluoromax-P.

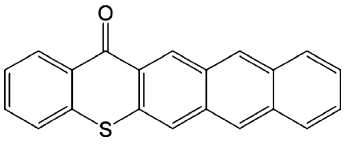


**Scheme 2.** Structure of thioxanthone–anthracene.

### 2.5. Real-time infrared spectroscopy photopolymerization studies [18,19]

Uniform samples of photocurable formulations consisting of a photoinitiator and multifunctional monomer; trimethylolpropane triacrylate (TMPTA) in the presence of MDEA were prepared by casting on a KBr pellet. The samples were placed in the compartment of a Fourier transform infrared spectrometer (Mattson 1000 FTIR) and were simultaneously exposed to a UV photolyzing light and an IR analyzing light beam. The photolyzing light was generated by a medium-pressure mercury lamp (Flexicure UV system) and was directed through a flexible fiber optic to the IR compartment.

The light intensity ($4.37 \times 10^{16}$ photons s$^{-1}$) was determined by potassium ferrioxalate actinometry. The spectrometer was operated in the absorbance mode, and the detection wavelength was set at 810 cm$^{-1}$ (C=C–H twist) to monitor the disappearance of double bonds. The degree of conversion, $\alpha$, can be expressed by the following relation:

$$\alpha = \frac{(A_0 - A_t)}{A_0} \quad (1)$$

where $A_0$ is the initial absorbance at 810 cm$^{-1}$ and $A_t$ the absorbance value at irradiation time $t$.

### 2.6. Photocalorimetry (Photo-DSC)

The photoinitiated polymerization of formulations of epoxyacrylate and tripropyleneglycoldiacrylate (EA + TPGDA) was carried out by TA-DSCQ100 equipped with a medium-pressure mercury arc lamp. This unit emits radiation predominantly in the 220–400 nm range, and provides light intensity of 40 mW cm$^{-2}$ as measured by a UV radiometer capable of broad UV range coverage. The mass of the samples was approximately 2 mg and the measurements were carried out in an isothermal mode at room temperature under a nitrogen atmosphere (nitrogen flow: 50 mL/min).

The samples were irradiated for 10 min at room temperature. The heat flux as a function of reaction time was monitored using DSC under isothermal conditions, and both the rate of polymerization and conversion were then calculated as a function of time. $\Delta H_p^{theor}$ is the theoretical heat for complete conversion of the monomer. $\Delta H_p^{theor}$ = 86 kJ/mol for acrylic double bonds [20]. Rates of polymerization were calculated according to the following equation:

$$R_p = \left(\frac{Q}{s}\right)\frac{M}{n}\Delta H_p m,$$

where $Q/s$ is heat flow per second, $M$ the molar mass of the monomer, $n$ the number of double bonds per monomer molecule and $m$ the mass of monomer in the sample.

## 3. Results and discussion

TX-Np was synthesized according to the literature procedure [16,17]. The structure of the photoinitiator was confirmed by spectral and elemental analysis (see Section 2). The absorption spectrum of TX-Np ($\varepsilon_{390}$ = 7500 L mol$^{-1}$ s$^{-1}$) was compared to the parent, thioxanthone. The absorption wavelength maxima of the initiator shifted to the visible region of the electromagnetic spectrum (Fig. 1).

The photodecomposition of TX-Np was followed by detecting spectral changes upon photolysis. The UV spectra of TX-Np in $CH_2Cl_2$ were recorded after the solution had been exposed to the light of the UV lamp at intervals of 90, 180, 480, 780, 1380, 1680, 1980 and 2280 s in air (Fig. 2). At the end of the irradiation (2280 s),

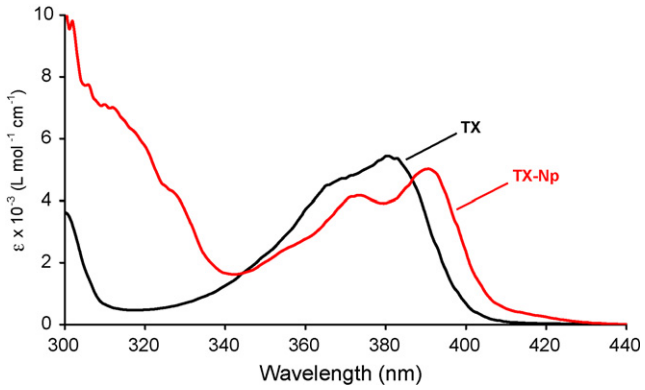


**Fig. 1.** Absorption spectra of TX-Np [$3.3 \times 10^{-4}$ M] and TX [$3.3 \times 10^{-4}$ M] in $CH_2Cl_2$.

the photoinitiator was consumed and the absorption bands of the thioxanthone moiety completely disappeared.

In order to clarify the mechanistic details, fluorescence and phosphorescence measurements were taken. The excitation spectrum of TX-Np (Fig. 3) is very similar to its UV–vis absorption spectrum (Fig. 1).

Fig. 3 shows that a nearly mirror-image-like relation exists between the absorption and emission of TX-Np. The singlet excited state energy of TX-Np, estimated from the intersection of the emission and excitation spectra at 400 nm, is ca. 299 kJ/mol. The fluorescence quantum yield ($\phi_f = 0.045$ for TX-Np) was estimated by using 9,10-diphenyl anthracene as the standard. ($\phi_f = 0.95$) [21,22].

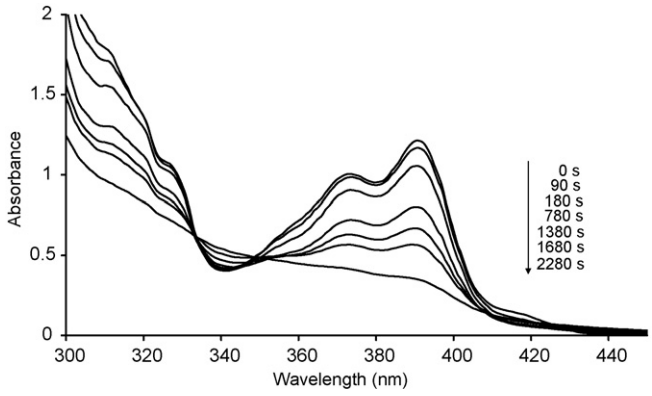


**Fig. 2.** Photobleaching of TX-Np [$1.6 \times 10^{-4}$ M] in $CH_2Cl_2$ during 0–2280 s in air atmosphere with polychromatic light (unfiltered light from a medium-pressure mercury lamp).

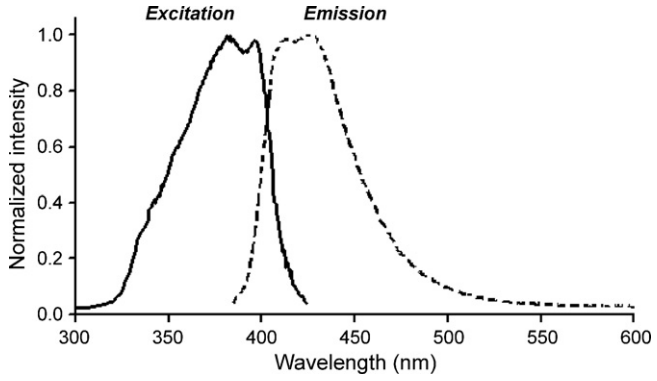


**Fig. 3.** Fluorescence excitation (—) and emission (---) spectra of thioxanthone–naphthalene (TX-Np) in $CH_2Cl_2$; $\lambda_{exc} = 380$ nm.

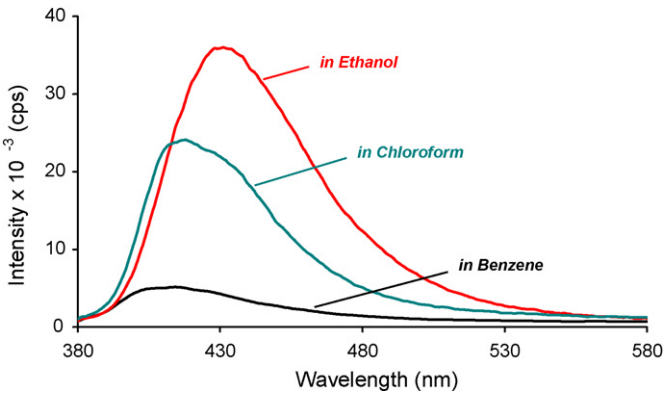


**Fig. 4.** Fluorescence emission spectra of TX-Np in various solvents; $\lambda_{exc} = 370$ nm.

The fluorescence emission spectrum of TX-Np was taken for solvents which have different polarities ($\lambda_{exc} = 370$ nm). As shown in Fig. 4, increasing the solvent polarity shifted the emission spectrum to the red. $\pi$–$\pi^*$ transitions are shifted to longer wavelengths by polar solvents, since the excited state may form stronger hydrogen bonds than the corresponding ground state. According to the emission spectra, when polarity increased, the transition shifted to longer wavelengths.

Phosphorescence measurements are useful to gain information on the triplet configuration of TX-Np (see Fig. 5). The phosphorescence lifetime for n–$\pi^*$ triplets is significantly shorter compared to $\pi$–$\pi^*$ triplets (more than 100 ms) [23–25].

Thus, the long phosphorescence lifetime, i.e. 197 ms in a matrix at 77 K in ethanol glass indicates a $\pi$–$\pi^*$ nature of the lowest triplet state for TX-Np. The (0,0) emission band for TX-Np occurs at 505 nm corresponding to the approximate triplet energy of ca. 237 kJ/mol.

Quenching experiments were performed by adding MDEA at different concentrations, and changes to the emission spectrum of the TX-Np solution were recorded. The Stern–Volmer representation (i.e. $I_o/I$ vs. [Q]) is shown in Fig. 6. It can be observed that the least squares fit of the experimental results produces a straight line with reasonable point scattering. The linearity of the corresponding plot was always excellent ($R^2 > 0.95$) and no deviation was detected at high quencher concentrations.

Photopolymerization experiments in air saturated $CH_2Cl_2$ solutions of MMA were performed using TX-Np as photoinitiator in the absence and presence of MDEA. The conversions of monomer (MMA) into polymer were determined gravimetrically and the results are shown in Tables 1 and 2.

Photopolymerization in an air atmosphere using TX-Np as initiator in the absence of MDEA yielded no polymer. Therefore, photopolymerization experiments for MMA with TX-Np were performed in the presence of MDEA with two different concentrations in $CH_2Cl_2$ and another set of experiments was performed under a nitrogen atmosphere (see Table 2).

**Table 1**
Photoinitiated polymerization of methyl methacrylate [MMA] in $CH_2Cl_2$ with TX-Np in the presence of MDEA in air atmosphere

| [TX-Np] (mol L$^{-1}$) | [TX] (mol L$^{-1}$) | Conversion[a] (%) | Conversion[b] (%) |
|---|---|---|---|
| $1.91 \times 10^{-3}$ | – | 5.50 | 7.80 |
| $4.73 \times 10^{-3}$ | – | 4.40 | 4.70 |
| $9.45 \times 10^{-3}$ | – | 2.50 | 3.60 |
| – | $1.91 \times 10^{-3}$ | 7.80 | 7.90 |

[MMA]: 4.68 mol L$^{-1}$. $t_{irr}$: 60 min.
[a] [MDEA]: $2.48 \times 10^{-2}$ mol L$^{-1}$.
[b] [MDEA]: $5.00 \times 10^{-2}$ mol L$^{-1}$.

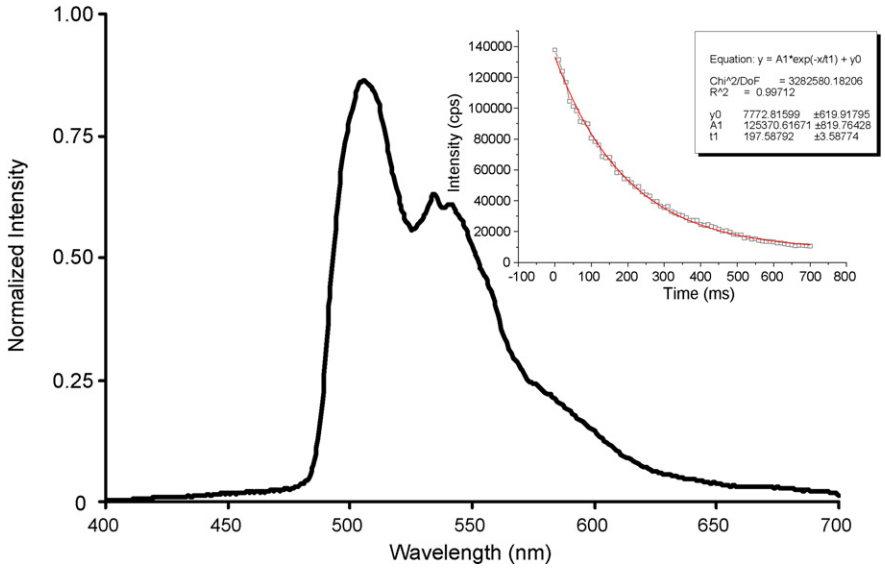


**Fig. 5.** Phosphorescence emission spectrum of TX-Np in $C_2H_5OH$ at 77 K.

It appears that as the concentration of TX-Np is increased, the extent of the polymerization decreases. This behaviour is due to the total absorption of irradiation by the photoinitiator and self-quenching of the excited photoinitiator at high concentrations (see Table 1).

As can be seen, the conversion percentage of MMA was lower in the presence of TX-Np and MDEA than the formulation containing TX and MDEA. When the amine concentration was increased, nearly doubled, the conversion percentage of MMA increased with a low concentration of TX-Np (see Table 1). The high activity of amines can be attributed to their ability to act as electron donors in the formation of exciplexes with triplet excited ketones, as well as to their high chain transfer reactivity for peroxide radicals and for acrylates.

The conversion percentage values obtained from the polymerization of MMA with TX-Np, which was performed under a nitrogen atmosphere, were found to be much lower than the formulation consisting of MDEA. Photoinitiated polymerization of MMA with TX-Np and TX in the presence of MDEA under a nitrogen atmosphere was also performed to see the effect of the sensitizer and the results were nearly the same for both of them.

For the possibility of using the described photoinitiator in practical applications, the efficiency of TX-Np in the photocuring of formulations containing multifunctional monomers was also studied. To investigate the polymerization kinetics, the disappearance of the monomer double bonds during the photocuring of the formulations was followed by Fourier transform real-time spectroscopy (RT-FTIR). By monitoring changes in the characteristic monomer IR absorption bands, it is possible to continuously follow the fast polymerization process. In Figs. 7 and 8 kinetic profiles referring to the polymerization of trimethylolpropanetriacrylate and EA and TPGDA under polychromatic light are shown. TX-Np/MDEA and TX/MDEA served as photoinitiators. The curves were obtained by monitoring the absorption decrease of the band at 810 $cm^{-1}$ corresponding to the frequency of the twisting vibration of the double bonds [18,19].

The shape of the curves indicates the existence of two polymerization stages: a rapid first stage which is followed by a slow stage. It can be seen that at early irradiation times, polymerization of TMPTA takes place with TX-Np/MDEA as efficiently as TX/MDEA. When the formulation consisted of TX-Np/MDEA/EA + TPGDA is subjected to further irradiation, a 70% conversion was achieved. As can be seen clearly from Fig. 4, TX-Np/MDEA is as efficient as TX/MDEA for formulations of both EA + TPGDA and TMPTA in prolonged irradiation times.

**Table 2**
Photoinitiated polymerization of MMA in $CH_2Cl_2$ with TX-Np under nitrogen atmosphere

| [TX] (mol $L^{-1}$) | [TX-Np] (mol $L^{-1}$) | [MDEA] (mol $L^{-1}$) | Conversion (%) |
|---|---|---|---|
| – | $1.91 \times 10^{-3}$ | – | 0.60 |
| – | $4.73 \times 10^{-3}$ | – | 1.10 |
| – | $9.45 \times 10^{-3}$ | – | 0.90 |
| – | $1.91 \times 10^{-3}$ | $5.00 \times 10^{-2}$ | 8.00 |
| $1.91 \times 10^{-3}$ | – | $5.00 \times 10^{-2}$ | 7.50 |

[MMA]: 4.68 mol $L^{-1}$. $t_{irr}$: 60 min.

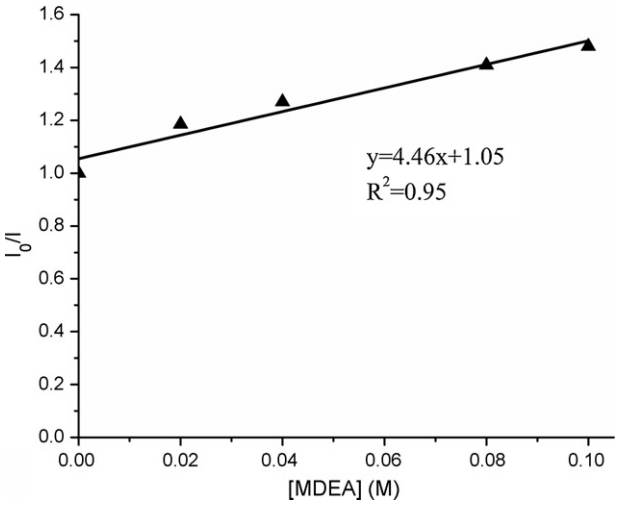


**Fig. 6.** Stern–Volmer plot of the quenching of TX-Np ($1.5 \times 10^{-4}$ mol $L^{-1}$) by MDEA in $CH_2Cl_2$ ($\lambda_{exc}$ = 380 nm). $I_o$ = fluorescence intensity of TX-Np, $I$ = fluorescence intensity in the presence of MDEA.

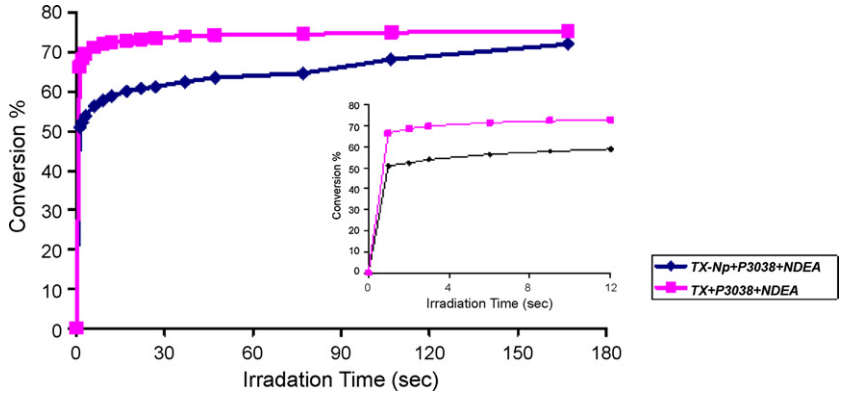


**Fig. 7.** Polymerization kinetics of epoxyacrylate and tripropyleneglycoldiacrylate (EA + TPGDA) with thioxanthone–naphthalene (TX-Np) (1, w/w%) and thioxanthone (TX) (1, w/w%) in the presence of *N*-methyldiethanolamine (MDEA) (10.0, w/w%) with polychromatic light (unfiltered light from a medium-pressure lamp) in an air atmosphere. The polymerization kinetics was measured as % loss of olefinic double bonds at 810 $cm^{-1}$ by IR spectroscopy. The inset shows the polymerization kinetics in the initial phase.

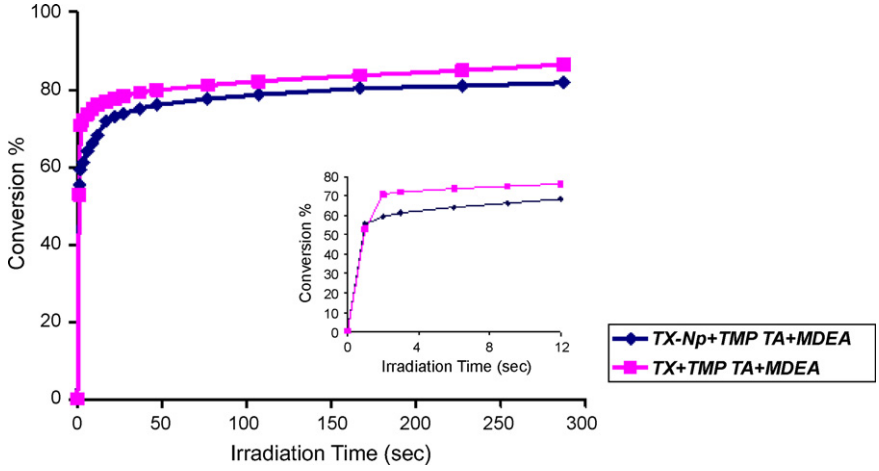


**Fig. 8.** Polymerization kinetics of trimethylpropanetriacrylate (TMPTA) with thioxanthone–naphthalene (TX-Np) (1, w/w%) and thioxanthone (TX) (1, w/w%) in the presence of *N*-methyldiethanolamine (MDEA) (10.0, w/w%) with polychromatic light (unfiltered light from a medium-pressure lamp) in an air atmosphere. The polymerization kinetics was measured as % loss of olefinic double bonds at 810 $cm^{-1}$ by IR spectroscopy. The inset shows the polymerization kinetics in the initial phase.

The photopolymerization kinetics of EA + TPGDA was performed by using Photo-DSC to clarify the effect of initiator on the photocuring process (Fig. 9).

Photo-DSC experiments are capable of providing kinetics data in which the measured heat flow can be converted directly to the ultimate percentage conversion and polymerization rate for a given amount of formulation, with the data obtained reflecting the overall curing reaction of the sample. As can be seen from Photo-DSC results (Fig. 9), TX-Np is as efficient as TX in the presence of MDEA.

Since MDEA is required for TX-Np to act as an initiator for acrylate polymerization, it is suggested that TX-Np reacts with MDEA to give α-aminoalkyl radicals which initiate polymerization as shown in Scheme 3. At the same time, MDEA scavenges oxygen and the α-aminoalkyl radical produced in the quenching cycle is also involved in the initiation process.

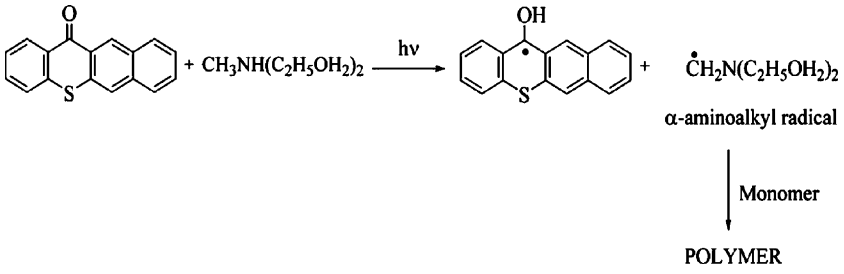


**Scheme 3.** General mechanism of Type II photoinitiation.

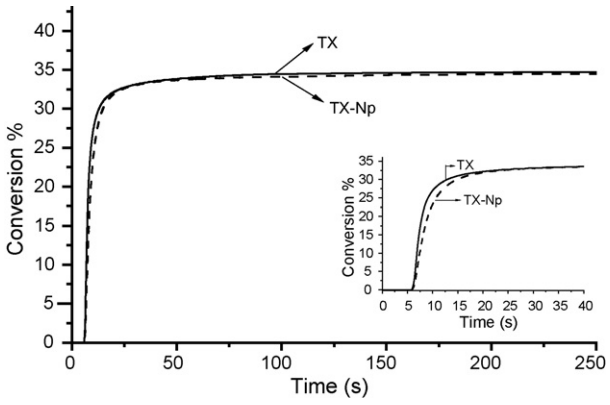


**Fig. 9.** Conversion vs. time for polymerization of EA + TPGDA initiated by TX-Np and TX cured by UV light with an intensity of 40 mW cm$^{-2}$. The inset shows the conversion vs. time for polymerization in the initial phase.

## 4. Conclusion

Photoinitiated polymerization of MMA with TX-Np in the presence of MDEA was performed and the obtained results were compared with the well-known Type II initiator, thioxanthone. According to the results, TX-Np can be classified as a Type II photoinitiator and the initiating efficiency of TX-Np is nearly the same as TX when MDEA was present in the formulation. In addition, excellent absorption properties of TX-Np suggest that it may find use in a variety of practical applications.

## Acknowledgement

The authors would like to thank TUBITAK, DPT and Yildiz Technical University Research Foundation for their financial support.

## References

[1] H.J. Timpe, S. Ulrich, C. Decker, J.P. Fouassier, Macromolecules 26 (17) (1993) 4560–4566.
[2] S.P. Pappas, UV Curing Science and Technology, Technology Marketing Corp., Norwalk, CA, 1978.
[3] A. Ledwith, M.D. Purbrich, Polymer 14 (1973) 521–522.
[4] R.S. Davidson, in: D. Bethel, V. Gold (Eds.), Advances in Physical Chemistry, Academic Press, London, 1983.
[5] A. Ledwith, J.A. Bosley, M.D. Purbric, J. Oil Colour Chem. Assoc. 61 (1978)95–104.
[6] J.P. Fouassier, Photoinitiation, Photopolymerization and Photocuring, Hanser Verlag, Munich, 1995.
[7] K. Dietliker, Chemistry & Technology of UV & EB Formulation for Coatings, Inks & Paints, vol. 3. Technology Ltd., London, SITA, 1991.
[8] R.S. Davidson, Exploring the Science, Technology and Applications of UV and EB Curing, SITA Technology Ltd., London, 1999.
[9] M.K. Mishra, Y. Yagci, Handbook of Radical Vinyl Polymerization, Marcel Dekker Inc., New York, 1998 (Chapter 7).
[10] M.J. Davis, J. Doherty, P.N. Godfrey, P.N. Gren, J.R.A. Yung, M.A. Parrish, J. Oil Colour Chem. Assoc. 11 (1978) 256–263.
[11] L. Cokbaglan, N. Arsu, Y. Yagci, S. Jockusch, N.J. Turro, Macromolecules 36 (8) (2003) 2649–2653.
[12] M. Aydin, N. Arsu, Y. Yagci, Macromol. Rapid Commun. 24 (12) (2003) 718–723.
[13] M. Aydin, N. Arsu, Y. Yagci, S. Jockusch, N.J. Turro, Macromolecules 38 (10) (2005) 4133–4138.
[14] G. Temel, N. Arsu, J. Photochem. Photobiol. A 191 (2–3) (2007) 149–152.
[15] D.K. Balta, N. Arsu, Y. Yagci, S. Jockusch, N.J. Turro, Macromolecules 40 (12) (2007) 4138–4141.
[16] F. Catalina, J.M. Tercero, C. Peinado, R. Sastre, J.L. Mateo, N.S. Allen, J. Photochem. Photobiol. A: Chem. 50 (1989) 249–258.
[17] R.H. Martin, N. Defay, F. Geerts-Evrard, P.H. Given, J.R. Jones, R.W. Wedel, Tetrahedron 21 (1965) 1833–1845.
[18] C. Decker, K. Moussa, Macromol. Chem. 189 (1988) 2381–2394.
[19] C. Decker, K. Moussa, Macromolecules 22 (1989) 4455–4462.
[20] X. Jiang, H. Xu, J. Yin, Polymer 45 (1) (2004) 133–140.
[21] J.V. Morris, M.A. Mahaney, J.R. Huber, J. Phys. Chem. 80 (1976) 969–974.
[22] J.C. Dalton, F.C. Montgomery, J. Am. Chem. Soc. 96 (1974) 6230–6232.
[23] N.J. Turro, Modern Molecular Photochemistry, University Science Books, Sausalito, CA, 1991.
[24] I. Carmichael, G.L. Hug, in: J.C. Scaiano (Ed.), CRC Handbook of Organic Photochemistry, vol. 1, CRC Press, Boca Raton, FL, 1989.
[25] X. Allonas, C. Ley, C. Bibaut, P. Jaques, J.P. Fouassier, Chem. Phys. Lett. 322 (2000) 483–490.